Chapter 4

# The Effect of Substituent on Molecules That Contain a Triple Bond Between Arsenic and Group 13 Elements: Theoretical Designs and Characterizations

Jia-Syun Lu, Ming-Chung Yang, Shih-Hao Su and Ming-Der Su

Additional information is available at the end of the chapter

http://dx.doi.org/10.5772/intechopen.69586

**Abstract**

The effect of substitution on the potential energy surfaces of $RE_{13}{\equiv}AsR$ ($E_{13}$ = group 13 elements; R = F, OH, H, $CH_3$, and $SiH_3$) is determined using density functional theory (M06-2X/Def2-TZVP,B3PW91/Def2-TZVP, and B3LYP/LANL2DZ+dp). The computational studies demonstrate that all triply bonded $RE_{13}{\equiv}AsR$ species prefer to adopt a bent geometry that is consistent with the valence electron model. The theoretical studies also demonstrate that $RE_{13}{\equiv}AsR$ molecules with smaller substituents are kinetically unstable, with respect to the intramolecular rearrangements. However, triply bonded $R'E_{13}{\equiv}AsR'$ species with bulkier substituents (R′ = SiMe(Si*t*$Bu_3)_2$, Si*i*$PrDis_2$, and NHC) are found to occupy the lowest minimum on the singlet potential energy surface, and they are both kinetically and thermodynamically stable. That is to say, the electronic and steric effects of bulky substituents play an important role in making molecules that feature an $E_{13}{\equiv}As$ triple bond as viable synthetic target.

**Keywords:** arsenic, group 13 elements, triple bond, density functional theory, multiple bond

## 1. Introduction

In the past two decades, studies that have been performed by many synthetic chemists have successfully synthesized and characterized homonuclear heavy alkyne-like $RE_{14}{\equiv}E_{14}R$ ($E_{14}$ = Si, Ge, Sn, and Pb) molecules [1–23]. Recently, heteronuclear ethyne-like compounds, $RC{\equiv}E_{14}R$, have also been experimentally studied [24, 25, 26] and theoretically predicted [27, 28, 29].

However, from the valence electron viewpoint, $RE_{13}{\equiv}E_{15}R$ ($E_{13}$ = group 13 elements and $E_{15}$ = group 15 elements) is isoelectronic with the $RE_{14}{\equiv}E_{14}R$ species. Therefore, triply bonded $RE_{13}{\equiv}E_{15}R$ is the next synthetic challenge. To the best of the authors' knowledge, only $R_2BN$ molecules that contain a B≡N triple bond have been experimentally demonstrated to exist [30–40].

## 2. Theoretical methods

This chapter reports the possible existence of triply bonded $RE_{13}{\equiv}AsR$ molecules, from the viewpoint of the effect of substituents, using density functional theories (DFT): M06-2X/Def2-TZVP, B3PW91/Def2-TZVP, and B3LYP/LANL2DZ+dp for small substituents and B3LYP/LANL2DZ+dp//RHF/3-21G* for large substituents. It is hoped that this theoretical study will stimulate further research into the synthetic chemistry of triply bonded $RE_{13}{\equiv}AsR$ species.

## 3. Results and discussion

### 3.1. Small ligands on substituted $RE_{13}{\equiv}AsR$

The effect of the electronegativity of six types of small substituents (R = F, OH, H, $CH_3$, and $SiH_3$) on the stability of the triply bonded $RE_{13}{\equiv}AsR$ molecules is determined using the three DFT methods. The molecular properties (geometrical parameters, singlet-triplet energy splitting, natural charge densities, binding energies (BE), and the Wiberg Bond Index (WBI)) are all listed in **Tables 1–5**. The reaction profiles for the unimolecular rearrangement reactions for the $RE_{13}{\equiv}AsR$ compounds are also given in **Figures 1–5**.

There are three noteworthy features of **Tables 1–5** and **Figures 1–5**.

1. From the tables, the three DFT calculations show that the triple bond distances (*Å*) for B≡As, Al≡As, Ga≡As, In≡As, and Tl≡As are estimated to be 1.835–1.908 (**Table 1**), 2.218–2.358 (**Table 2**), 2.239–2.364 (**Table 3**), 2.404–2.546 (**Table 4**), and 2.426–2.570 (**Table 5**). As previously mentioned, no experimental values for these triple bond lengths have been reported, so these computational data are a prediction.
2. In **Tables 1–5**, these DFT computations all demonstrate that the triply bonded $RE_{13}{\equiv}AsR$ molecules favor a bent structure, rather than a linear structure. This is explained by the bonding model, as shown in **Figure 6**. Because there is a significant difference between the sizes of the valence s and p atomic orbitals in the As atom, hybrid orbitals between the valence *s* and *p* orbitals are not easily formed (the so-called orbital non-hybridization effect or the inert s-pair effect) [41–44]. Therefore, $RE_{13}{\equiv}AsR$ molecules that have a heavier As center are predicted to favor a bent angle $\angle E_{13}$–As–R (close to 90°). The DFT computational data that are shown in **Tables 1–5** confirm this prediction.

| R | F | OH | H | CH3 | SiH3 |
|---|---|---|---|---|---|
| **B≡As (Å)** | 1.901 | 1.892 | 1.837 | 1.839 | 1.814 |
| | (1.898) | (1.888) | (1.835) | (1.839) | (1.820) |
| | [1.908] | [1.906] | [1.849] | [1.861] | [1.839] |
| **∠R–B–As (°)** | 177.2 | 179.5 | 178.1 | 175.1 | 175.3 |
| | (177.8) | (179.5) | (174.6) | (175.1) | (172.4) |
| | [177.0] | [179.1] | [177.5] | [174.3] | [174.8] |
| **∠B–As–R (°)** | 93.03 | 92.73 | 81.22 | 94.69 | 68.92 |
| | (92.71) | (92.21) | (89.39) | (94.69) | (68.98) |
| | [92.39] | [92.95] | [78.37] | [96.15] | [72.25] |
| **∠R–B–As–R (°)** | 180.0 | 179.8 | 180.0 | 179.8 | 148.7 |
| | (180.0) | (180.0) | (180.0) | (179.8) | (180.0) |
| | [180.0] | [176.2] | [179.0] | [176.3] | [179.4] |
| $Q_B$[1] | 0.354 | 0.184 | −0.017 | −0.007 | 0.037 |
| | (0.262) | (0.108) | (−0.028) | (−0.057) | (0.036) |
| | [0.232] | [0.070] | [−0.106] | [−0.160] | [−0.407] |
| $Q_{As}$[2] | 0.243 | 0.080 | −0.152 | −0.073 | −0.085 |
| | (0.255) | (0.097) | (−0.134) | (−0.040) | (−0.017) |
| | [0.238] | [0.086] | [0.034] | [−0.035] | [0.030] |
| **BE (kcal mol$^{-1}$)**[3] | 63.56 | 56.97 | 114.7 | 94.39 | 79.90 |
| | (63.34) | (60.28) | (120.1) | (137.6) | (74.75) |
| | [57.45] | [55.28] | [113.7] | [132.6] | [73.79] |
| **WBI**[4] | 1.800 | 1.830 | 2.141 | 2.027 | 2.204 |
| | (1.813) | (1.823) | (2.158) | (2.029) | (2.168) |
| | [1.835] | [1.836] | [2.135] | [2.041] | [2.185] |

1 The natural charge density on the B atom.

2 The natural charge density on the As atom.

3 BE = E(triplet state for R–B) + E(triplet state for R–As) − E(singlet state for RB≡AsR).

4 The Wiberg bond index (WBI) for the B–As bond: see [45, 46].

**Table 1.** The main geometrical parameters, the singlet-triplet energy splitting ($\Delta E_{ST}$), the natural charge densities ($Q_B$ and $Q_{As}$), the binding energies (BE), and the Wiberg Bond Index (WBI) for RB≡AsR using the M06-2X/Def2-TZVP, B3PW91/Def2-TZVP (in round brackets), and B3LYP/LANL2DZ+dp (in square brackets) levels of theory.

| R | F | OH | H | CH3 | SiH3 |
|---|---|---|---|---|---|
| **Al≡As (Å)** | 2.327 | 2.321 | 2.218 | 2.253 | 2.227 |
| | (2.325) | (2.323) | (2.221) | (2.256) | (2.236) |
| | [2.355] | [2.358] | [2.269] | [2.285] | [2.292] |
| **∠R–Al–As (°)** | 178.6 | 174.4 | 172.5 | 172.8 | 168.4 |
| | (179.5) | (174.3) | (172.2) | (172.0) | (167.3) |
| | [178.8] | [173.9] | [177.5] | [171.1] | [173.7] |
| **∠Al–As–R (°)** | 93.07 | 91.08 | 66.95 | 98.77 | 91.93 |
| | (93.51) | (92.45) | (67.45) | (100.7) | (95.83) |
| | [90.64] | [90.97] | [75.97] | [100.5] | [90.36] |
| **∠R–Al–As–R (°)** | 180.0 | 180.0 | 180.0 | 174.2 | 174.7 |
| | (179.8) | (178.5) | (179.6) | (176.8) | (175.7) |
| | [180.0] | [179.0] | [178.0] | [174.5] | [176.8] |
| $Q_{Al}$[1] | 0.555 | 0.4574 | 0.2401 | 0.293 | 0.291 |
| | (0.530) | (0.443) | (0.234) | (0.280) | (0.313) |
| | [0.784] | [0.540] | [0.504] | [0.353] | [0.245] |
| $Q_{As}$[2] | 0.158 | 0.015 | −0.276 | −0.170 | −0.262 |
| | (0.142) | (−0.007) | (−0.246) | (−0.156) | (−0.209) |
| | [0.056] | [−0.032] | [−0.209] | [−0.284] | [−0.290] |
| **BE (kcal mol$^{-1}$)**[3] | 33.90 | 28.23 | 71.86 | 56.47 | 53.22 |
| | (38.90) | (31.24) | (77.42) | (60.57) | (54.98) |
| | [33.89] | [25.68] | [69.27] | [52.63] | [67.74] |
| **WBI**[4] | 1.532 | 1.523 | 1.714 | 1.649 | 1.647 |
| | (1.567) | (1.553) | (1.742) | (1.679) | (1.675) |
| | [1.557] | [1.545] | [1.714] | [1.690] | [1.550] |

1 The natural charge density on the Al atom.

2 The natural charge density on the As atom.

3 BE = E(triplet state for R–Al) + E(triplet state for R–As) − E(singlet state for RAl≡AsR).

4 The Wiberg bond index (WBI) for the Al–As bond: see [45, 46].

**Table 2.** The main geometrical parameters, the singlet-triplet energy splitting ($\Delta E_{ST}$), the natural charge densities ($Q_{Al}$ and $Q_{As}$), the binding energies (BE), and the Wiberg Bond Index (WBI) for RAl≡AsR using the M06-2X/Def2-TZVP, B3PW91/Def2-TZVP (in round brackets), and B3LYP/LANL2DZ+dp (in square brackets) levels of theory.

**3.** In terms of the stability of the $RE_{13}$≡AsR species, the three DFT computations are used to study the energy surfaces for the $RE_{13}$≡AsR systems, and the theoretical results are shown in **Figures 1–5**. These figures show three local minima (i.e., $R_2E_{13}$=As, $RE_{13}$≡AsR, and $E_{13}$=$AsR_2$) and two saddle points that connect them. It is seen that regardless of the type of small substituent, triply bonded $RE_{13}$≡AsR molecules are unstable on the potential energy surfaces, so they easily undergo a 1,2-migration reaction to produce the most stable doubly bonded isomers. There is strong theoretical evidence that there is no possibility of observing triply bonded $RE_{13}$≡AsR compounds in transient intermediates or even in a matrix.

http://dx.doi.org/10.5772/intechopen.69586

### 3.2. Large ligands on substituted R′$E_{13}$≡AsR′

Bulky substituents are used to determine the possible existence of triply bonded R′$E_{13}$≡AsR′ (R′= SiMe(Si*t*Bu$_3$)$_2$, Si*i*PrDis$_2$, and NHC; (**Scheme 1**)) molecules. The molecular properties, the natural bond orbital (NBO) [45, 46], and the natural resonance theory (NRT) [47, 48, 49] analyses of R′$E_{13}$≡AsR′ are computed at the B3LYP/LANL2DZ+dp//RHF/3-21G* level of theory, and the results are shown in **Tables 6**, **7** (R′B≡AsR′), **8**, **9** (R′Al≡AsR′), **10**, **11** (R′Ga≡AsR′), **12**, **13** (R′In≡AsR′), and **14** and **15** (R′Tl≡AsR′).

| R | F | OH | H | CH3 | SiH3 |
|---|---|---|---|---|---|
| **Ga≡As (Å)** | 2.261 | 2.339 | 2.239 | 2.330 | 2.243 |
| | (2.319) | (2.314) | (2.224) | (2.243) | (2.242) |
| | [2.364] | [2.364] | [2.263] | [2.285] | [2.270 |
| **∠R–Ga–As (°)** | 179.5 | 173.2 | 176.2 | 169.9 | 168.5 |
| | (178.5) | (177.4) | (178.6) | (173.6) | (179.1) |
| | [179.3] | [176.2] | [179.1] | [171.1] | [179.2] |
| **∠Ga–As–R (°)** | 92.80 | 93.16 | 76.00 | 103.0 | 93.43 |
| | (94.36) | (94.54) | (79.18) | (99.37) | (73.64) |
| | [91.81] | [93.68] | [80.30] | [100.4] | [76.86] |
| **∠R–Ga–As–R (°)** | 180.0 | 175.6 | 179.6 | 175.7 | 173.5 |
| | (180.0) | (178.1) | (179.1) | (178.4) | (175.6) |
| | [173.1] | [177.4] | [178.2] | [174.5] | [178.1] |
| $Q_{Ga}$[1] | 0.7067 | 0.592 | 0.310 | 0.4451 | 0.3352 |
| | (0.554) | (0.410) | (0.215) | (0.260) | (0.241) |
| | [0.706] | [0.474] | [0.435] | [0.295] | [0.174] |
| $Q_{As}$[2] | 0.0899 | −0.047 | −0.374 | −0.256 | −0.3697 |
| | (0.154) | (0.023) | (−0.262) | (−0.151) | (−0.222) |
| | [0.133] | [0.006] | [−0.184] | [−0.246] | [−0.284] |
| **BE (kcal mol$^{-1}$)**[3] | 28.56 | 23.82 | 67.79 | 53.57 | 49.26 |
| | (30.61) | (25.96) | (71.91) | (58.12) | (51.77) |
| | [27.65] | [90.75] | [65.14] | [50.32] | [62.24] |
| **WBI**[4] | 1.476 | 1.498 | 1.691 | 1.648 | 1.646 |
| | (1.486) | (1.503) | (1.717) | (1.652) | (1.596) |
| | [1.487] | [1.495] | [1.707] | [1.668] | [1.615] |

1 The natural charge density on the Ga atom.

2 The natural charge density on the As atom.

3 BE = E(triplet state for R–Ga) + E(triplet state for R–As) − E(singlet state for RGa≡AsR).

4 The Wiberg bond index (WBI) for the Ga–As bond: see [45, 46].

**Table 3.** The main geometrical parameters, the singlet-triplet energy splitting ($\Delta E_{ST}$), the natural charge densities ($Q_{Ga}$ and $Q_{As}$), the binding energies (BE), and the Wiberg Bond Index (WBI) for RGa≡AsR using the M06-2X/Def2-TZVP, B3PW91/Def2-TZVP (in round brackets), and B3LYP/LANL2DZ+dp (in square brackets) levels of theory.

| R | F | OH | H | CH3 | SiH3 |
|---|---|---|---|---|---|
| **In≡As (Å)** | 2.511 | 2.512 | 2.412 | 2.431 | 2.411 |
| | (2.495) | (2.497) | (2.399) | (2.418) | (2.404) |
| | [2.535] | [2.546] | [2.432] | [2.459] | [2.444] |
| **∠R–In–As (°)** | 179.9 | 178.8 | 179.3 | 173.6 | 170.9 |
| | (179.9) | (176.9) | (179.9) | (173.3) | (168.4) |
| | [177.8] | [175.2] | [179.8] | [172.5] | [167.4] |
| **∠In–As–R (°)** | 92.32 | 95.31 | 81.43 | 99.72 | 93.85 |
| | (93.86) | (96.11) | (82.67) | (100.4) | (99.59) |
| | [91.08] | [94.22] | [82.28] | [100.5] | [102.0] |
| **∠R–In–As–R (°)** | 180.0 | 169.3 | 177.3 | 174.7 | 177.1 |
| | (180.0) | (166.8) | (175.9) | (173.0) | (177.4) |
| | [180.0] | [163.8] | [179.6] | [179.8] | [178.2] |
| $Q_{In}$[1] | 1.288 | 1.233 | 1.012 | 1.144 | 0.8840 |
| | (1.196) | (1.123) | (0.912) | (1.037) | (0.7881) |
| | [1.343] | [1.287] | [1.076] | [1.121] | [0.9682] |
| $Q_{As}$[2] | 0.138 | 0.036 | −0.624 | −0.388 | −0.767 |
| | (0.146) | (0.047) | (−0.571) | (−0.335) | (−0.703) |
| | [0.077] | [−0.005] | [−0.591] | [−0.367] | [−0.748] |
| **BE (kcal mol$^{-1}$)**[3] | 22.14 | 18.30 | 55.63 | 53.87 | 57.82 |
| | (19.72) | (20.13) | (60.95) | (50.24) | (57.34) |
| | [24.06] | [16.22] | [57.18] | [53.36] | [54.39] |
| **WBI**[4] | 1.536 | 1.551 | 1.773 | 1.719 | 1.726 |
| | (1.546) | (1.554) | (1.798) | (1.738) | (1.749) |
| | [1.572] | [1.562] | [1.780] | [1.729] | [1.710] |

1 The natural charge density on the In atom.

2 The natural charge density on the As atom.

3 BE = E(triplet state for R–In) + E(triplet state for R–As) − E(singlet state for RIn≡AsR).

4 The Wiberg bond index (WBI) for the In–As bond, see [45, 46].

**Table 4.** The main geometrical parameters, the singlet-triplet energy splitting ($\Delta E_{ST}$), the natural charge densities ($Q_{In}$ and $Q_{As}$), the binding energies (BE), and the Wiberg Bond Index (WBI) for RIn≡AsR using the M06-2X/Def2-TZVP, B3PW91/Def2-TZVP (in round brackets), and B3LYP/LANL2DZ+dp (in square brackets) levels of theory.

http://dx.doi.org/10.5772/intechopen.69586

| R | F | OH | H | CH3 | SiH3 |
|---|---|---|---|---|---|
| **Tl≡As (Å)** | 2.535 | 2.531 | 2.426 | 2.446 | 2.431 |
| | (2.533) | (2.536) | (2.428) | (2.450) | (2.432) |
| | [2.558] | [2.570] | [2.429] | [2.459] | [2.433] |
| **∠R–Tl–As (°)** | 179.9 | 178.2 | 180.0 | 176.6 | 176.5 |
| | (179.9) | (175.8) | (179.5) | (175.0) | (173.4) |
| | [179.2] | [177.0] | [179.5] | [173.8] | [177.7] |
| **∠Tl–As–R (°)** | 91.49 | 94.88 | 84.22 | 97.14 | 90.08 |
| | (93.64) | (96.73) | (84.51) | (99.33) | (93.68) |
| | [92.21] | [96.20] | [84.07] | [99.33] | [89.37] |
| **∠R–Tl–As–R (°)** | 180.0 | 175.5 | 173.0 | 178.0 | 179.2 |
| | (179.3) | (176.7) | (178.1) | (178.2) | (178.5) |
| | [180.0] | [172.9] | [179.6] | [177.6] | [177.2] |
| $Q_{Tl}$[1] | 0.736 | 0.640 | 0.3883 | 0.482 | 0.3051 |
| | (0.656) | (0.538) | (0.352) | (0.428) | (0.382) |
| | [0.817] | [0.549] | [0.472] | [0.361] | [0.244] |
| $Q_{As}$[2] | 0.190 | 0.035 | −0.4169 | −0.251 | −0.3290 |
| | (0.163) | (0.013) | (−0.351) | (−0.208) | (−0.291) |
| | [0.139] | [0.021] | [−0.204] | [−0.273] | [−0.336] |
| **BE (kcal mol$^{-1}$)**[3] | 13.48 | 10.36 | 50.28 | 38.25 | 29.93 |
| | (16.73) | (13.88) | (55.13) | (43.44) | (30.60) |
| | [15.13] | [8.720] | [49.40] | [37.22] | [45.10] |
| **WBI**[4] | 1.109 | 1.148 | 1.456 | 1.382 | 1.409 |
| | (1.143) | (1.174) | (1.492) | (1.416) | (1.407) |
| | [1.168] | [1.175] | [1.484] | [1.413] | [1.411] |

1 The natural charge density on the Tl atom.

2 The natural charge density on the As atom.

3 BE = E(triplet state for R–Tl) + E(triplet state for R–As) − E(singlet state for RTl≡AsR).

4 The Wiberg bond index (WBI) for the Tl–As bond, see [45, 46].

**Table 5.** The main geometrical parameters, the singlet-triplet energy splitting ($\Delta E_{ST}$), the natural charge densities ($Q_{Tl}$ and $Q_{As}$), the binding energies (BE), and the Wiberg Bond Index (WBI) for RTl≡AsR using the M06-2X/Def2-TZVP, B3PW91/Def2-TZVP (in round brackets), and B3LYP/LANL2DZ+dp (in square brackets) levels of theory.

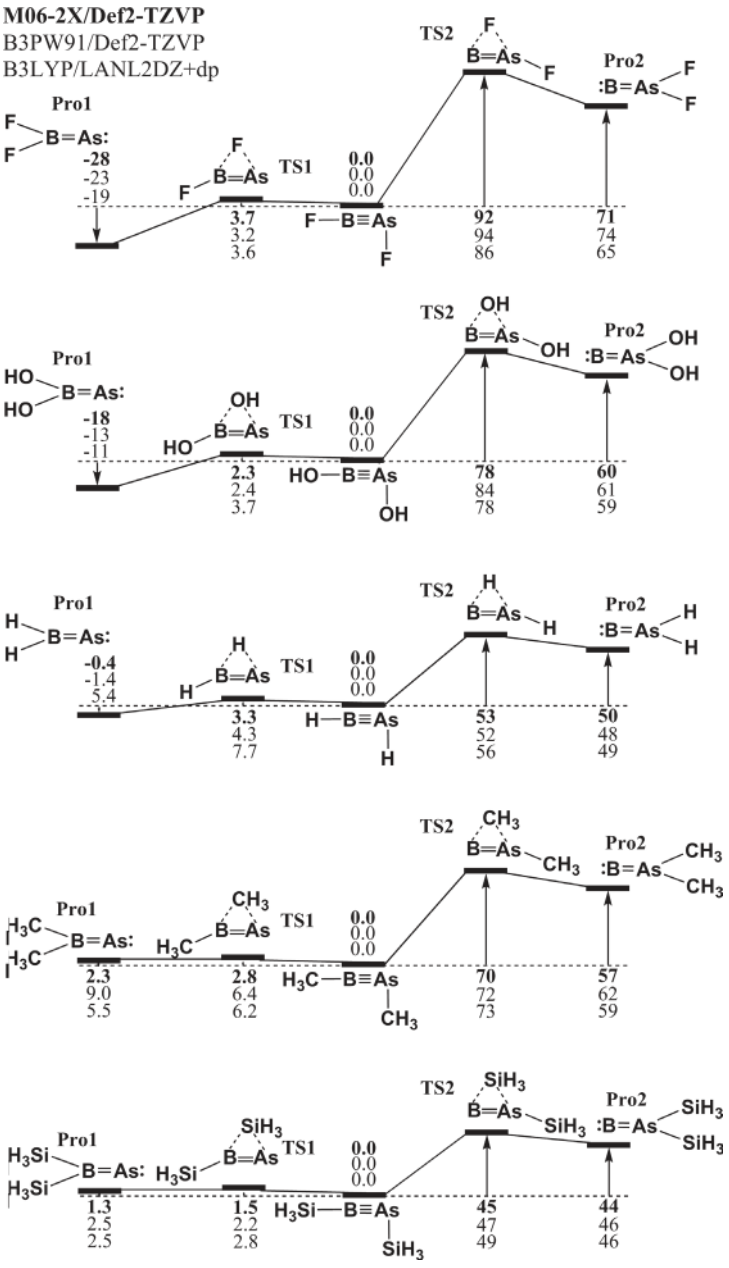


**Figure 1.** The relative Gibbs free energies for RB ≡ AsR (R = F, OH, H, $CH_3$, and $SiH_3$). All energies are in kcal/mol and are calculated at the M06-2X/Def2-TZVP, B3PW91/Def2-TZVP, and B3LYP/LANL2DZ+dp levels of theory.

http://dx.doi.org/10.5772/intechopen.69586

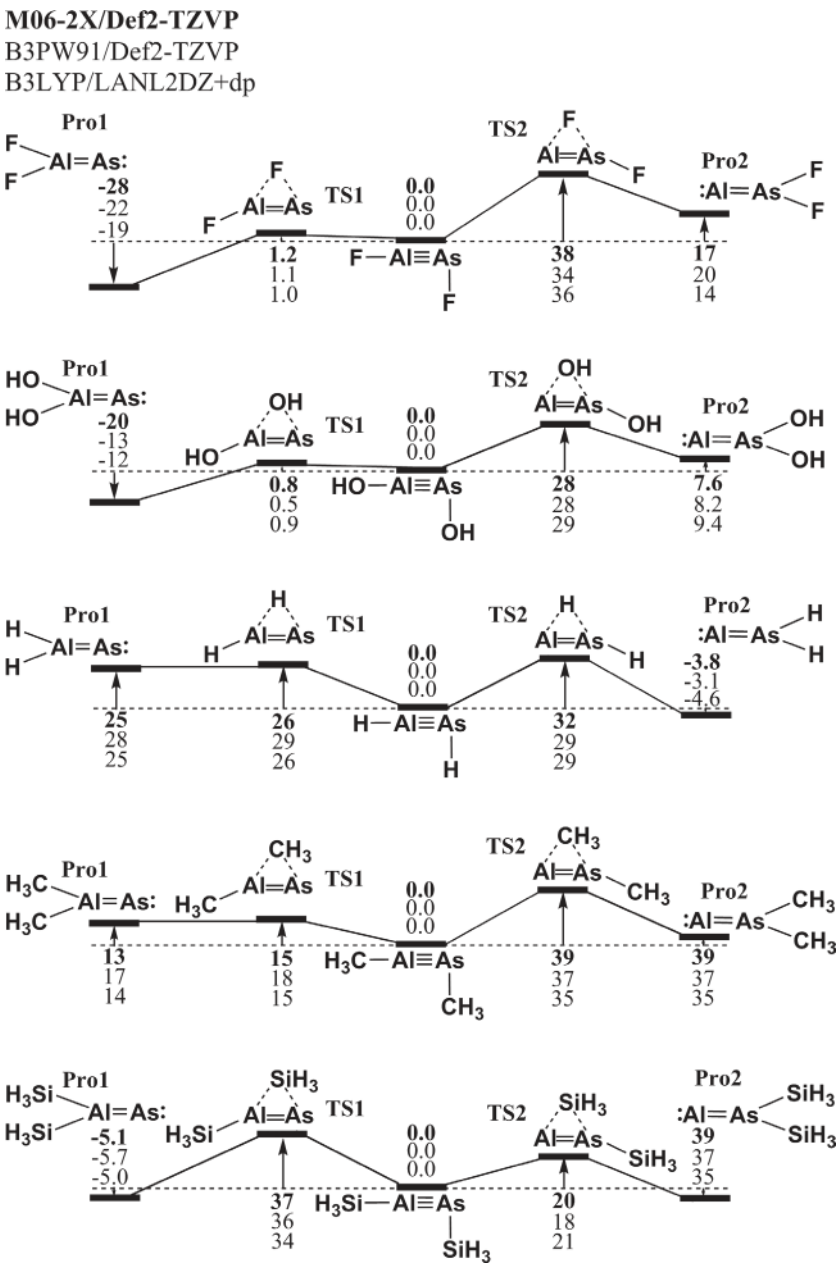


**Figure 2.** The relative Gibbs free energies for RAl≡AsR (R = F, OH, H, $CH_3$, and $SiH_3$). All energies are in kcal/mol and are calculated at the M06-2X/Def2-TZVP, B3PW91/Def2-TZVP, and B3LYP/LANL2DZ+dp levels of theory.

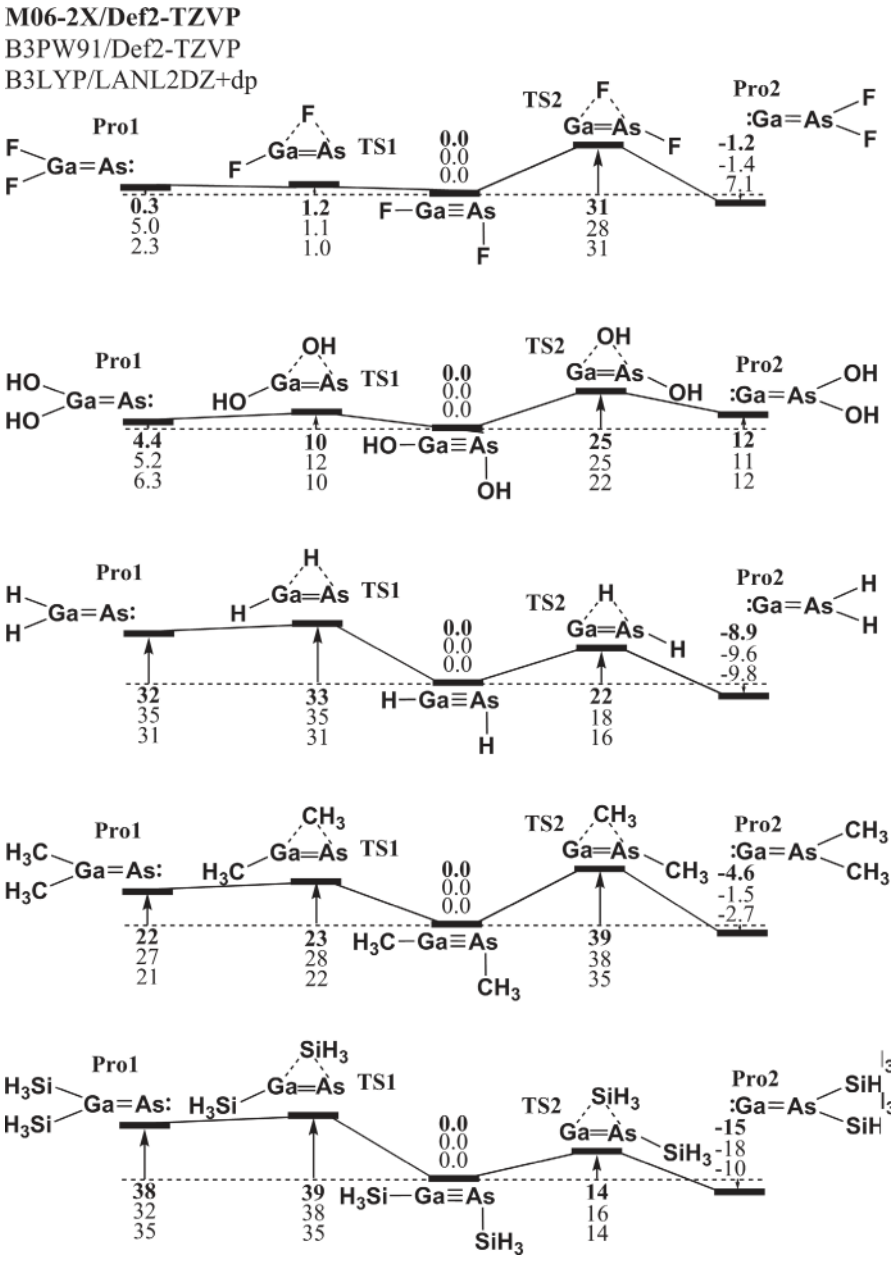


**Figure 3.** The relative Gibbs free energies for RGa ≡ AsR (R = F, OH, H, $CH_3$, and $SiH_3$). All energies are in kcal/mol and are calculated at the M06-2X/Def2-TZVP, B3PW91/Def2-TZVP, and B3LYP/LANL2DZ+dp levels of theory.

http://dx.doi.org/10.5772/intechopen.69586

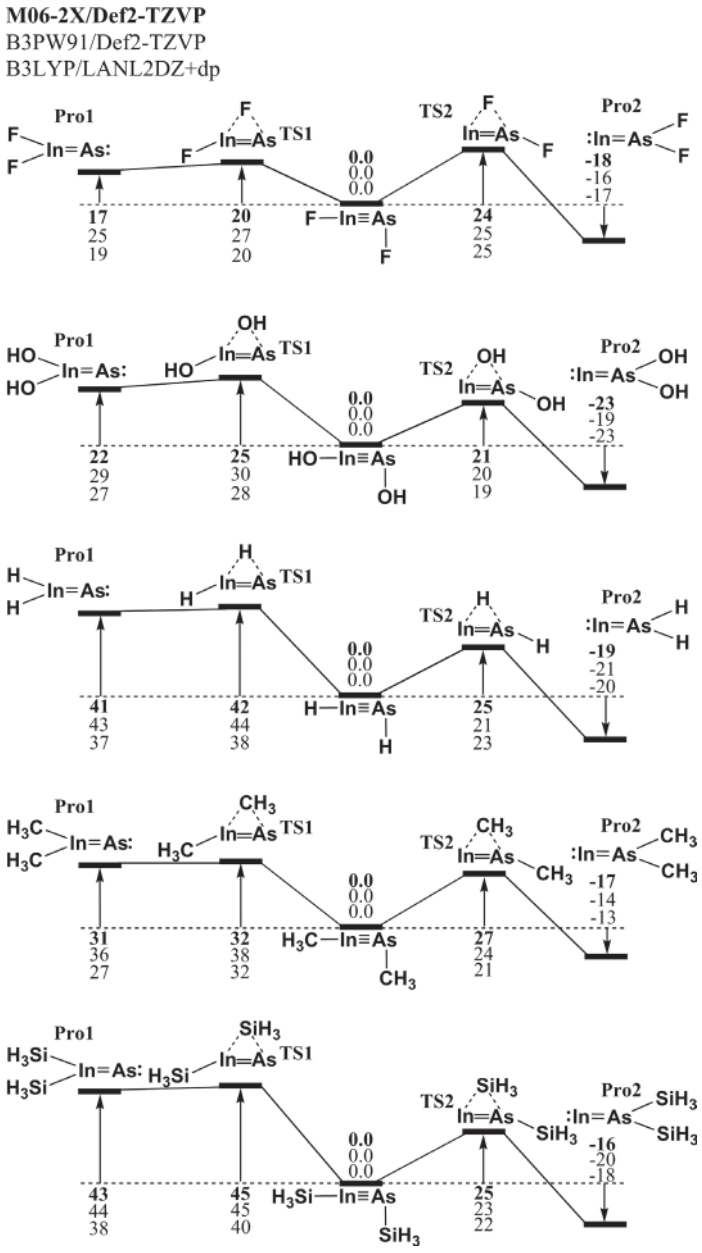


**Figure 4.** The relative Gibbs free energies for RIn≡AsR (R = F, OH, H, $CH_3$, and $SiH_3$). All energies are in kcal/mol and are calculated at the M06-2X/Def2-TZVP, B3PW91/Def2-TZVP, and B3LYP/LANL2DZ+dp levels of theory.

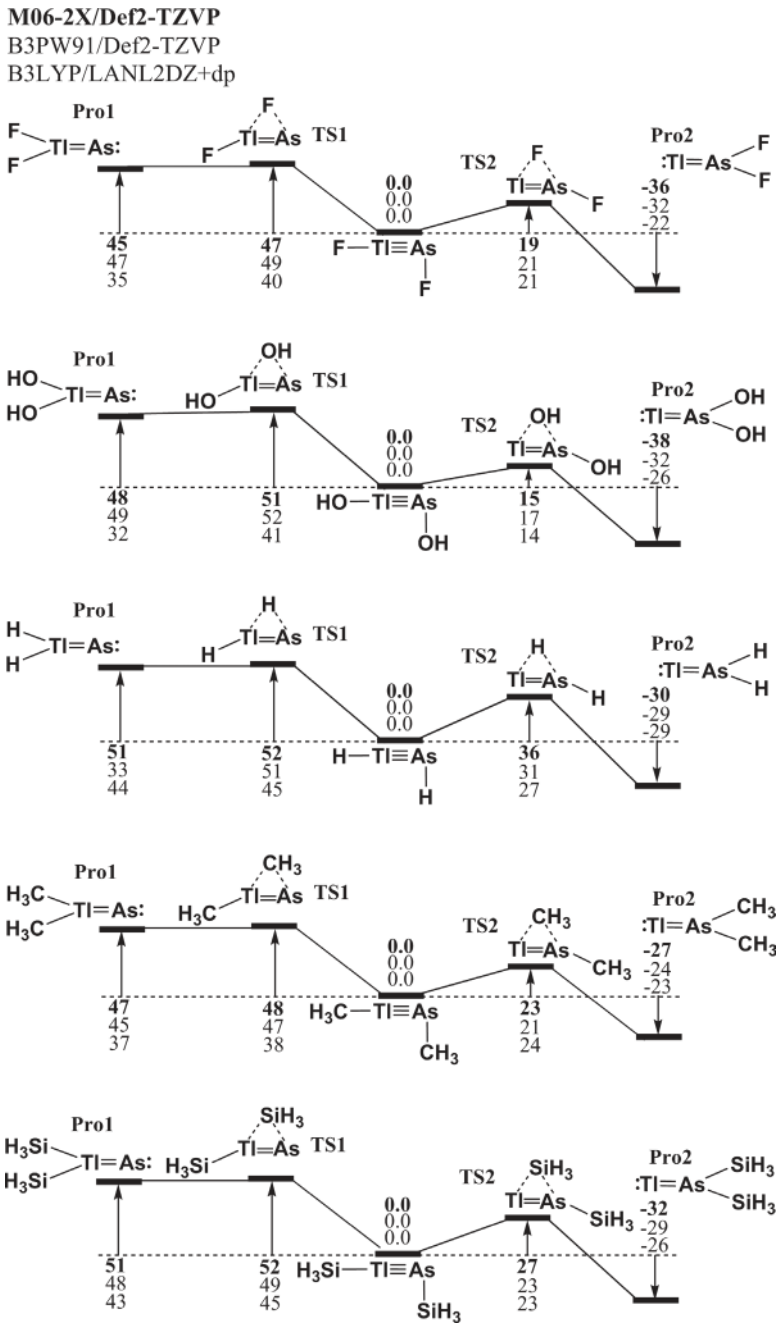


**Figure 5.** The relative Gibbs free energies for RTl≡AsR (R = F, OH, H, $CH_3$, and $SiH_3$). All energies are in kcal/mol and are calculated at the M06-2X/Def2-TZVP, B3PW91/Def2-TZVP, and B3LYP/LANL2DZ+dp levels of theory.

http://dx.doi.org/10.5772/intechopen.69586

The results in **Tables 6–15** allow three conclusions to be drawn.

1. The calculations that are shown in **Tables 6** (B), **8** (Al), **10** (Ga), **12** (In), and **14** (Tl) show that the computed $E_{13}$≡As triple bond distances (*Å*) for these bulkily substituted species (R'$E_{13}$≡AsR') are estimated to be 1.821–1.837 (B≡As), 2.257–2.307 (Al≡As), 2.252–2.316 (Ga≡As), 2.430–2.482 (In≡As), and 2.565–2.653 (Tl≡As). The values for the WBO that are shown in **Tables 6–10** (for bulky ligands) are obviously greater than those that are shown in **Tables 1–5** (for smaller ligands). These WBO values show that bulkier substituents increase the bond order for the $E_{13}$≡As triple bond length.
2. Similarly to the results for small ligands, the computational results show that R'$E_{13}$≡AsR' species that feature large substituents all adopt a bent conformation. This phenomenon is explained by bonding model (II), which is shown in **Figure 6**.
3. The NBO values that are shown in **Tables 7** (B≡As), **9** (Al≡As), **11** (Ga≡As), **13** (In≡As), and **15** (Tl≡As) show that the acetylene-like R'$E_{13}$≡AsR' compounds feature a weak triple bond. For example, the B3LYP/LANL2DZ+dp data for the NBO analyses of the B≡As π bonding in (Si*i*PrDis$_2$–B≡As–Si*i*PrDis$_2$), which shows that NBO(B≡As) = $0.5880(2s2p^{99.99})$ B + $0.8089(4s4p^{1.00})$As, provide strong evidence that the predominant bonding interaction between the B–Si*i*PrDis$_2$ and the As–Si*i*PrDis$_2$ units results from 2p(B) ← 4p(As) donation, whereby boron's electron deficiency and π bond polarity are partially balanced by the donation of the arsenic lone pair into the empty boron *p* orbital to develop a hybrid π bond. The polarization analyses using the NBO model again demonstrate the presence of the B≡As π bonding orbital, 34.58% of which is composed of natural B orbitals and 65.42% of which is natural As orbitals. **Table 7** also shows that the B≡As triple bond in (Si*i*PrDis$_2$–B≡As–Si*i*PrDis$_2$) has a shorter single bond character (6.04%) and a shorter triple bond character (36.74%), but a greater double bond character (57.2%), because the ionic part of the NRT bond order (0.53) is shorter than its covalent part (1.71). The same theoretical observations are also seen for the other two differently substituted R'B≡AsR' compounds, as shown in **Table 7**, and in the data for the other R'$E_{13}$≡BiR' compounds that is shown in **Tables 9 (Al)**, **11 (Ga)**, **13 (In)**, and **15 (Tl)**. These computational data demonstrate that these R'$E_{13}$≡AsR' molecules have a weak $E_{13}$≡As triple bond.

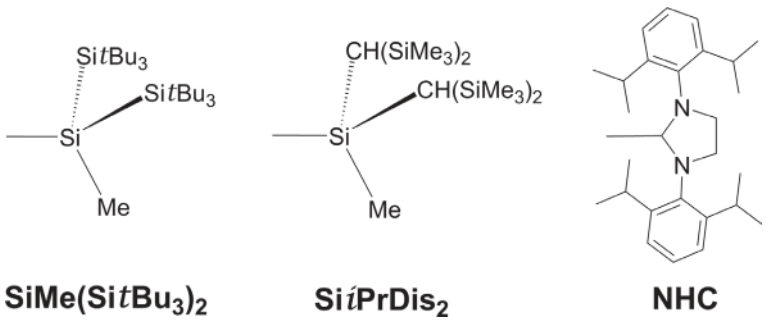


**Scheme 1.** Three bulky ligands: SiMe(Si*t*Bu$_3$)$_2$, Si*i*PrDis$_2$, and N-heterocyclic carbine.

| R′ | SiMe(Si*t*Bu$_3$)$_2$ | Si*i*PrDis$_2$ | NHC |
|---|---|---|---|
| **B≡As (Å)** | 1.837 | 1.821 | 1.819 |
| **∠R′–B–As (°)** | 177.2 | 172.9 | 174.5 |
| **∠B–As–R′ (°)** | 128.2 | 121.6 | 111.2 |
| **∠R′–B–As–R′ (°)** | 179.6 | 177.4 | 171.5 |
| $Q_B$[1] | −0.280 | −0.397 | −0.205 |
| $Q_{As}$[2] | −0.228 | −0.134 | 0.061 |
| **$\Delta E_{ST}$ (kcal mol$^{-1}$)**[3] | 94.42 | 75.22 | 83.64 |
| **Wiberg BO**[4] | 2.327 | 2.395 | 2.254 |

1 The natural charge density on the central B atom.

2 The natural charge density on the central As atom.

3 BE = E (triplet state for B–R′) + E (triplet state for As–R′) − E (singlet state for R′B≡AsR′).

4 The Wiberg bond index (WBI) for the B–As bond.

5 $\Delta H_1$ = E (:B=AsR′$_2$) − E (R′B≡AsR′); see Scheme 2.

6 $\Delta H_2$ = E (R′$_2$B=As:) − E (R′B≡AsR′); see Scheme 2.

**Table 6.** The geometrical parameters, natural charge densities ($Q_B$ and $Q_{As}$), Binding Energies (BE), the HOMO-LUMO Energy Gaps, the Wiberg Bond Index (WBI), and some reaction enthalpies for R′B≡AsR′ at the B3LYP/LANL2DZ+dp//RHF/3-21G* Level of Theory.

| R′B≡AsR′ | WBI | NBO analysis | | | NRT analysis | |
|---|---|---|---|---|---|---|
| | | Occupancy | hybridization | Polarization | total/covalent/ionic | Resonance weight |
| R′ = SiMe(Si*t*Bu$_3$)$_2$ | 2.31 | σ = 1.98 | σ : 0.6627 B (sp$^{1.46}$) + 0.7489 As (sp$^{1.07}$) | 43.91% (B) 56.09% (As) | 2.35/1.66/0.69 | B–As: 5.68% B=As: 60.70% B≡As: 33.62% |
| | | π = 1.94 | π : 0.5941 B (sp$^{1.00}$) + 0.8044 As (sp$^{99.99}$) | 35.29% (B) 64.71% (As) | | |
| R′ = Si*i*PrDis2 | 2.27 | σ = 1.98 | σ : 0.6630 B (sp$^{1.54}$) + 0.7486 As (sp$^{1.22}$) | 43.96% (B) 56.04% (As) | 2.24/1.71/0.53 | B–As: 6.04% B=As : 57.2% B=As : 36.74% |
| | | π = 1.94 | π : 0.5880 B (sp$^{99.99}$) + 0.8089 As (sp$^{99.99}$) | 34.58% (B) 65.42% (As) | | |
| R′ = NHC | 2.26 | σ = 1.98 | σ : 0.6918 B (sp$^{0.90}$) + 0.7221 As (sp$^{2.66}$) | 47.86% (B) 52.14% (As) | 2.23/1.52/0.71 | B–As : 7.05% B=As : 69.13% B≡As : 23.82% |
| | | π = 1.94 | π : 0.5899 B (sp$^{99.99}$) + 0.8075 As (sp$^{99.99}$) | 34.80% (B) 65.20% (As) | | |

**Table 7.** Selected results for the natural bond orbital (NBO) and natural resonance theory (NRT) analyses at the B3LYP/LANL2DZ+dp level of theory for R′B≡AsR′ compounds that have large substituents.

http://dx.doi.org/10.5772/intechopen.69586

| R′ | $SiMe(SitBu_3)_2$ | $SiiPrDis_2$ | NHC |
|---|---|---|---|
| **Al≡As (Å)** | 2.285 | 2.257 | 2.307 |
| **∠R′–Al–As (°)** | 179.4 | 176.0 | 174.5 |
| **∠Al–As–R′ (°)** | 116.4 | 118.7 | 113.0 |
| **∠R′–Al–As–R′ (°)** | 176.1 | 170.6 | 176.4 |
| $Q_{Al}$ [1] | 0.3771 | 0.3120 | 0.4392 |
| $Q_{As}$ [2] | −0.5579 | −0.4907 | −0.3144 |
| **$\Delta E_{ST}$ (kcal mol$^{-1}$)[3]** | 44.64 | 54.23 | 34.53 |
| **Wiberg BO[4]** | 2.171 | 2.184 | 2.185 |

1 The natural charge density on the central Al atom.

2 The natural charge density on the central As atom.

3 BE = E(triplet state for Al–R′) + E(triplet state for As–R′) − E(singlet state for R′Al≡AsR′).

4 The Wiberg bond index (WBI) for the Al–As bond.

5 $\Delta H_1$ = E(:Al=AsR′$_2$) − E(R′Al≡AsR′); see Scheme 2.

6 $\Delta H_2$ = E(R′$_2$Al=As:) − E(R′Al≡AsR′); see Scheme 2.

**Table 8.** The geometrical parameters, natural charge densities ($Q_{Al}$ and $Q_{As}$), binding energies (BE), the HOMO-LUMO energy gaps, the Wiberg Bond Index (WBI), and some reaction enthalpies for R′Al≡AsR′ at the B3LYP/LANL2DZ+dp//RHF/3-21G* level of theory.

| R′Al≡AsR′ | WBI | NBO analysis | | | NRT analysis | |
|---|---|---|---|---|---|---|
| | | Occupancy | hybridization | Polarization | total/covalent/ionic | Resonance weight |
| R′ = $SiMe(SitBu_3)_2$ | 2.21 | σ = 1.92 | σ : 0.5080 Al ($sp^{1.59}$) + 0.8614 As ($sp^{1.14}$) | 25.81% (Al) 74.19% (As) | 2.24/1.66/0.58 | Al–As : 6.51% Al=As : 70.32% Al≡As : 23.17% |
| | | π = 1.92 | π : 0.4437 Al ($sp^{99.99}$) + 0.8962 As ($sp^{99.99}$) | 19.69% (Al) 80.31% (As) | | |
| R′ = $SiiPrDis2$ | 2.29 | σ = 1.92 | σ : 0.4956 Al ($sp^{1.84}$) + 0.8685 As ($sp^{1.06}$) | 24.57% (Al) 75.43% (As) | 2.27/1.73/0.54 | Al–As: 4.52% Al≡As : 57.55% Al≡As : 37.93% |
| | | π = 1.91 | π : 0.4383 Al ($sp^{99.99}$) + 0.8988 As ($sp^{99.99}$) | 19.21% (Al) 80.79% (As) | | |
| R′ = NHC | 2.36 | σ = 1.87 | σ : 0.5834 Al ($sp^{0.99}$) + 0.8122 As ($sp^{10.87}$) | 34.04% (Al) 65.96% (As) | 2.30/1.59/0.71 | Al–As : 6.61% Al=As : 74.90% Al=As : 18.49% |
| | | π = 1.94 | π : 0.4408 Al ($sp^{90.78}$) + 0.8976 As ($sp^{99.99}$) | 19.43% (Al) 80.57% (As) | | |

**Table 9.** Selected results for the natural bond orbital (NBO) and natural resonance theory (NRT) analyses at the B3LYP/LANL2DZ+dp level of theory for R′Al≡AsR′ compounds that have large substituents.

| R′ | $SiMe(SitBu_3)_2$ | $SiiPrDis_2$ | NHC |
|---|---|---|---|
| **Ga≡As (Å)** | 2.274 | 2.252 | 2.316 |
| **∠R′–Ga–As (°)** | 178.8 | 178.1 | 171.9 |
| **∠Ga–As–R′ (°)** | 119.3 | 122.8 | 114.5 |
| **∠R′–Ga–As–R′ (°)** | 176.6 | 171.0 | 176.5 |
| $Q_{Ga}$[1] | 0.1760 | 0.09195 | 0.2133 |
| $Q_{As}$[2] | −0.4683 | −0.3978 | −0.2257 |
| **$\Delta E_{ST}$ (kcal mol$^{-1}$)**[3] | 40.67 | 31.52 | 33.97 |
| **Wiberg BO**[4] | 2.125 | 2.174 | 2.154 |

1 The natural charge density on the central Ga atom.

2 The natural charge density on the central As atom.

3 BE = E(triplet state for Ga–R′) + E(triplet state for As–R′) − E(singlet state for R′Ga≡AsR′).

4 The Wiberg bond index (WBI) for the Ga–As bond.

5 $\Delta H_1$ = E(:Ga=AsR′$_2$) − E(R′Ga≡AsR′); see Scheme 2.

6 $\Delta H_2$ = E(R′$_2$Ga=As:) − E(R′Ga≡AsR′); see Scheme 2.

**Table 10.** The geometrical parameters, natural charge densities ($Q_{Ga}$ and $Q_{As}$), binding energies (BE), the HOMO-LUMO energy gaps, the Wiberg Bond Index (WBI), and some reaction enthalpies for R′Ga≡AsR′ at the B3LYP/LANL2DZ+dp//RHF/3-21G* level of theory.

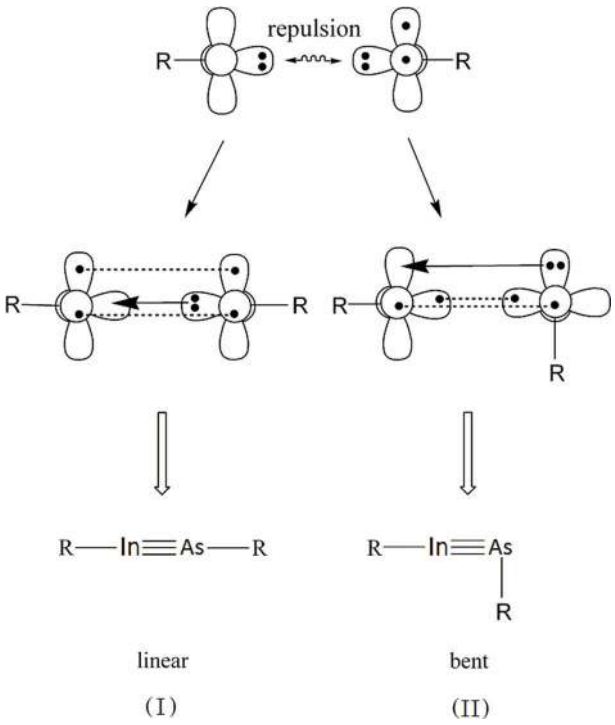


**Figure 6.** The bonding models (I) and (II) for the triply bonded $RE_{13}$≡AsR molecule.

http://dx.doi.org/10.5772/intechopen.69586

| R′Ga≡AsR′ | WBI | NBO analysis | | | NRT analysis | |
|---|---|---|---|---|---|---|
| | | Occupancy | Hybridization | Polarization | total/covalent/ ionic | Resonance weight |
| R′ = SiMe(Si*t*Bu$_3$)$_2$ | 2.19 | σ = 1.90 | σ : 0.5320 Ga (sp$^{1.52}$) + 0.8468 As (sp$^{1.32}$) | 28.30% (Ga) 71.70% (As) | 2.27/1.62/0.65 | Ga–As : 4.72% Ga=As : 56.61% Ga≡As : 38.67% |
| | | π = 1.93 | π : 0.4467 Ga (sp$^{99.99}$) + 0.8947 As (sp$^{99.99}$) | 19.95% (Ga) 80.05% (As) | | |
| R′ = Si*i*PrDis2 | 2.25 | σ = 1.91 | σ : 0.5386 Ga (sp$^{1.49}$) + 0.8426 As (sp$^{1.46}$) | 29.01% (Ga) 70.99% (As) | 2.31/1.64/0.67 | Ga–As : 7.03% Ga=As : 68.13% Ga≡As : 24.84% |
| | | π = 1.92 | π : 0.4392 Ga (sp$^{99.99}$) + 0.8984 As (sp$^{99.99}$) | 19.29% (Ga) 80.71% (As) | | |
| R′ = NHC | 2.33 | σ = 1.85 | σ : 0.6076 Ga (sp$^{0.98}$) + 0.7942 As (sp$^{12.06}$) | 36.92% (Ga) 63.08% (As) | 2.14/1.71/0.43 | Ga–As : 7.12% Ga=As : 75.34% Ga≡As : 17.54% |
| | | π = 1.93 | π : 0.4370 Ga (sp$^{82.50}$) + 0.8995 As (sp$^{99.99}$) | 19.09% (Ga) 80.91% (As) | | |

**Table 11.** Selected results for the natural bond orbital (NBO) and natural resonance theory (NRT) analyses at the B3LYP/LANL2DZ+dp level of theory for R′Ga≡AsR′ compounds that have large substituents.

| R′ | SiMe(Si*t*Bu$_3$)$_2$ | Si*i*PrDis$_2$ | NHC |
|---|---|---|---|
| **In≡As (Å)** | 2.446 | 2.430 | 2.482 |
| **∠R′–In–As (°)** | 155.9 | 168.4 | 171.3 |
| **∠In–As–R′ (°)** | 127.8 | 120.3 | 110.8 |
| **∠R′–In–As–R′ (°)** | 173.9 | 162.0 | 168.3 |
| $Q_{In}$[1] | 0.874 | 0.880 | 1.021 |
| $Q_{As}$[2] | −0.783 | −0.822 | −0.359 |
| **$\Delta E_{ST}$ (kcal mol$^{-1}$)**[3] | 41.5 | 45.2 | 35.7 |
| **Wiberg BO**[4] | 2.174 | 2.271 | 2.141 |

1 The natural charge density on the central In atom.

2 The natural charge density on the central As atom.

3 BE = E(triplet state for In–R′) + E(triplet state for As–R′) − E(singlet state for R′In≡AsR′).

4 The Wiberg bond index (WBI) for the In–As bond.

5 $\Delta H_1$ = E(:In=AsR′$_2$) – E(R′In≡AsR′); see Scheme 2.

6 $\Delta H_2$ = E(R′$_2$In=As:) − E(R′In≡AsR′); see Scheme 2.

**Table 12.** The geometrical parameters, natural charge densities ($Q_{In}$ and $Q_{As}$), Binding Energies (BE), the HOMO-LUMO Energy Gaps, the Wiberg Bond Index (WBI), and some reaction enthalpies for R′In≡AsR′ at the B3LYP/LANL2DZ+dp//RHF/3-21G* Level of Theory.

| R′In≡AsR′ | WBI | NBO analysis | | | NRT analysis | |
|---|---|---|---|---|---|---|
| | | Occupancy | Hybridization | Polarization | total/covalent/ ionic | Resonance weight |
| R′ = SiMe(Si*t*Bu$_3$)$_2$ | 1.50 | σ = 1.87 | σ : 0.4940 In ($sp^{1.58}$) + 0.8695 As ($sp^{1.28}$) | 24.41% (In) 75.59% (As) | 2.31/1.55/0.76 | In–As : 5.78% In=As :55.2 % In=As : 39.0% |
| | | π = 1.85 | π : 0.4411 In ($sp^{2.80}$) + 0.8975 As ($sp^{4.33}$) | 19.45% (In) 80.55% (As) | | |
| R′ = Si*i*PrDis2 | 1.48 | σ = 1.87 | σ : 0.4854 In ($sp^{1.71}$) + 0.8743 As ($sp^{1.26}$) | 23.56% (In) 76.44% (As) | 2.18/1.62/0.56 | In–As : 6.01% In=As : 56.29% In=As : 37.70% |
| | | π = 1.83 | π : 0.3873 In ($sp^{99.99}$) + 0.9220 As ($sp^{1.00}$) | 15.00% (In) 85.00% (As) | | |
| R′ = NHC | 1.33 | σ = 1.80 | σ : 0.5709 In ($sp^{1.07}$) + 0.8210 As ($sp^{8.66}$) | 32.60% (In) 67.40% (As) | 2.21/1.48/0.73 | In–As : 7.72% In=As : 78.30% In=As : 13.98% |
| | | π = 1.94 | π : 0.4805 In ($sp^{37.19}$) + 0.8770 As ($sp^{14.95}$) | 23.09% (In) 76.91% (As) | | |

**Table 13.** Selected results for the natural bond orbital (NBO) and natural resonance theory (NRT) analyses at the B3LYP/LANL2DZ+dp level of theory for R′In≡AsR′ compounds that have large substituents.

| R′ | SiMe(Si*t*Bu$_3$)$_2$ | Si*i*PrDis$_2$ | NHC |
|---|---|---|---|
| **Tl≡As (Å)** | 2.615 | 2.565 | 2.653 |
| **∠R′–Tl–As (°)** | 176.9 | 177.6 | 178.7 |
| **∠Tl–As–R′ (°)** | 127.7 | 121.8 | 108.0 |
| **∠R′–Tl–As–R′ (°)** | 172.2 | 170.4 | 175.2 |
| **$Q_{Tl}$**[1] | 0.310 | 0.246 | 0.262 |
| **$Q_{As}$**[2] | −0.462 | −0.440 | −0.313 |
| **$\Delta E_{ST}$ (kcal mol$^{-1}$)**[3] | 45.07 | 32.71 | 34.83 |
| **Wiberg BO**[4] | 2.157 | 2.214 | 2.209 |

1 The natural charge density on the central Tl atom.

2 The natural charge density on the central As atom.

3 BE = E(triplet state for Tl–R′) + E(triplet state for As–R′) − E(singlet state for R′Tl≡AsR′).

4 The Wiberg bond index (WBI) for the Tl–As bond.

5 $\Delta H_1$ = E(:Tl=AsR′$_2$) − E(R′Tl≡AsR′); see Scheme 2.

6 $\Delta H_2$ = E(R′$_2$Tl=As:) – E(R′Tl≡AsR′); see Scheme 2.

**Table 14.** The geometrical parameters, natural charge densities ($Q_{Tl}$ and $Q_{As}$), Binding Energies (BE), the HOMO-LUMO Energy Gaps, the Wiberg Bond Index (WBI), and some reaction enthalpies for R′Tl≡AsR′ at the B3LYP/LANL2DZ+dp//RHF/3-21G* Level of Theory.

http://dx.doi.org/10.5772/intechopen.69586

| R′Tl≡AsR′ | WBI | NBO analysis | | | NRT analysis | |
|---|---|---|---|---|---|---|
| | | Occupancy | Hybridization | Polarization | total/covalent/ ionic | Resonance weight |
| R′ = $SiMe(SitBu_3)_2$ | 2.15 | σ = 1.74 | σ : 0.5404 Tl ($sp^{1.51}$) + 0.8414 As ($sp^{2.20}$) | 29.20% (Tl) 70.80% (As) | 2.24/1.68/0.56 | Tl–As : 6.11% Tl=As : 57.27% Tl=As : 36.62% |
| | | π = 1.79 | π : 0.3968 Tl ($sp^{4.25}$) + 0.9179 As ($sp^{1.51}$) | 15.74% (Tl) 84.26% (As) | | |
| R′ = SiiPrDis2 | 2.21 | σ = 1.90 | σ : 0.3627 Tl ($sp^{38.20}$) + 0.9318 As ($sp^{1.44}$) | 13.16% (Tl) 86.84% (As) | 2.16/1.73/0.43 | Tl–As : 7.01% Tl=As : 66.48% Tl=As : 26.51% |
| | | π = 1.94 | π : 0.3315 Tl ($sp^{99.99}$) + 0.9435 As ($sp^{1.00}$) | 10.99% (Tl) 89.01% (As) | | |
| R′ = NHC | 2.11 | σ = 1.97 | σ : 0.7814 Tl ($sp^{0.07}$) + 0.6240 As ($sp^{52.63}$) | 61.06% (Tl) 38.94% (As) | 2.14/1.71/0.43 | Tl–As : 6.71% Tl=As : 75.51% Tl=As : 17.78% |
| | | π = 1.97 | π : 0.4726 Tl ($sp^{57.71}$) + 0.8812 As ($sp^{17.96}$) | 22.34% (Tl) 77.66% (As) | | |

**Table 15.** Selected results for the natural bond orbital (NBO) and natural resonance theory (NRT) analyses at the B3LYP/LANL2DZ+dp level of theory for R′Tl≡AsR′ compounds that have large substituents.

## 4. Conclusion

This study of the effect of substituents on the possibility of the existence of triply bonded $RE_{13}$≡AsR allows the following conclusions to be drawn (**Scheme 2**):

1. The theoretical observations provide strong evidence that bonding mode (B) is dominant in the triply bonded $RE_{13}$≡BiR species, because their structures are bent due to electron transfer (denoted by arrows in **Figure 1**) and the relativistic effect, which increases stability.

2. The theoretical evidence shows that both the electronic and the steric effects of substituents are crucial to rendering the $E_{13}$≡As triple bond synthetically accessible. However, this theoretical study shows that these $E_{13}$≡As triple bonds are weak. They are not as strong as the traditional C≡C triple bond. The results of this theoretical study show that triply bonded R′$E_{13}$≡AsR′ molecules that feature bulky substituents are more stable because bulky substituents not only protect the central $E_{13}$≡As triple bond because there is large steric hindrance but also prohibit polymerization reactions.

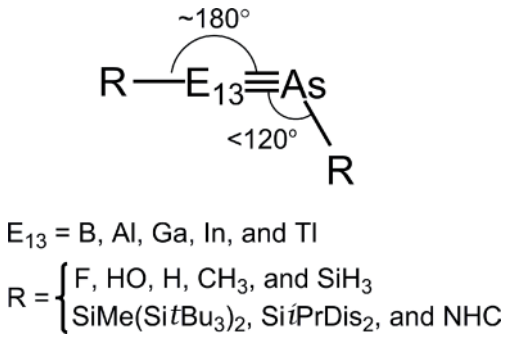


**Scheme 2.** The predicted structure for the triply bonded $RE_{13}{\equiv}AsR$ molecules based on the present theoretical computations.

## Acknowledgements

The authors are grateful to the National Center for High-Performance Computing of Taiwan in providing huge computing resources to facilitate this research. They also thank the Ministry of Science and Technology of Taiwan for the financial support.

## Author details

Jia-Syun Lu[1], Ming-Chung Yang[1], Shih-Hao Su[1] and Ming-Der Su[1,2]*

*Address all correspondence to: midesu@mail.ncyu.edu.tw

1 Department of Applied Chemistry, National Chiayi University, Chiayi, Taiwan

2 Department of Medicinal and Applied Chemistry, Kaohsiung Medical University, Kaohsiung, Taiwan

## References

[1] Power PP. π-Bonding and the lone pair effect in multiple bonds between heavier main group elements. Chemical Review. 1999;**99**:3463-3504

[2] Jutzi P. Stable system with a triple bond to silicon or its homologues: Another challenge. Angewandte Chemie International Edition. 2000;**39:**3797-3800

[3] Weidenbruch M. Some recent advances in the chemistry of silicon and its homologues in low coordination states. Journal of Organometallic Chemistry. 2002;**646**:39-352

[4] Power PP. Silicon, germanium, tin and lead analogues of acetylenes. Chemical Communications. 2003;**17**:2091-2101

[5] Power PP. Synthesis and some reactivity studies of germanium, tin and lead analogues of alkynes. Applied Organometallic Chemistry. 2005;**19:**488-493

[6] Lein M, Krapp A, Frenking G. Why do the heavy-atom analogues of acetylene E2H2 (E = Si-Pb) exhibit unusual structures? Journal of the American Chemical Society. 2005;**127**:6290-6299

[7] Sekiguchi A, Ichinohe M, Kinjo R. The chemistry of disilyne with a genuine si–si triple bond: Synthesis, structure, and reactivity. Bulletin of the Chemical Society of Japan. 2006;**79**:825-832

[8] Power PP. Bonding and reactivity of heavier group 14 element alkyne analogues. Organometallics. 2007;**26**:4362-4372

[9] Sekiguchi, A. Disilyne with a silicon-silicon triple bond: A new entry to multiple bond chemistry. Pure and Applied Chemistry. 2008;**80**:447-457

[10] Sekiguchi A, Kinjo R, Ichinohe M. Interaction of π-bonds of the silicon–silicon triple bond with alkali metals: An isolable anion radical upon reduction of a disilyne. Synthetic Metals. 2009;**159**:773-775

[11] Fischer RC, Power PP. π-bonding and the lone pair effect in multiple bonds involving heavier main group elements: Developments in the new millennium. Chemical Review. 2010;**110**:3877-3923

[12] Peng Y, Fischer RC, Merrill WA, Fischer J, Pu L, Ellis BD, Fettinger JC, Herber RH, Power PP. Substituent effects in ditetrel alkyne analogues: Multiple vs. single bonded isomers. Chemical Science. 2010;**1**:461-468

[13] Sasamori T, Han J S, Hironaka K, Takagi N, Nagase S, Tokitoh N. Synthesis and structure of stable 1,2-diaryldisilyne. Pure and Applied Chemistry. 2010;**82**:603-612

[14] Sekiguchi A, Kinjo R, Ichinohe M. A stable compound containing a silicon-silicon triple bond. Science. 2004;**305**:1755-1757

[15] Wiberg N, Vasisht S K, Fischer G, Mayer P. Disilynes. iii [1] a relatively stable disilyne RSi≡SiR (R = $SiMe(SitBu_3)_2$). Zeitschrift für anorganische und allgemeine Chemie. 2004;**630**:1823-1828

[16] Sasamori T, Hironaka K, Sugiyama T, Takagi N, Nagase S, Hosoi Y, Furukawa Y, Tokitoh N. Synthesis and reactions of a stable 1,2-diaryl-1,2-dibromodisilene: A precursor for substituted disilenes and 1,2-diaryldisilyne. Journal of the American Chemical Society. 2008;**130**:13856-13857

[17] Stender M, Phillips AD, Wright RJ, Power PP. Synthesis and characterization of a digermanium analogue of an alkyne. Angewandte Chemie International Edition. 2002; **41**:1785-1787

[18] Stender M, Phillips AD, Power PP. Formation of $[Ar^*Ge\{CH_2C(Me)C(Me)CH_2\}CH_2C(Me)N]_2$ ($Ar^* = C_6H_3$-2,6-$Trip_2$; $Trip = C_6H_2$-2,4,6-*i*-$Pr_3$) via reaction of Ar*GeGeAr* with 2,3-dimethyl-1,3-butadiene: Evidence for the existence of a Germanium analogue of an alkyne. Chemical Communication. 2002;**12**:1312-1313

[19] Pu L, Phillips AD, Richards AF, Stender M, Simons RS, Olmstead MM, Power PP. Germanium and tin analogues of alkynes and their reduction products. Journal of the American Chemical Society. 2003;**125**:11626-11636

[20] Sugiyama Y, Sasamori T, Hosoi Y, Furukawa Y, Takagi N, Nagase S, Tokitoh N. Synthesis and properties of a new kinetically stabilized digermyne: New insights for a germanium analogue of an alkyne. Journal of the American Chemical Society. 2006;**128**:1023-1031

[21] Spikes GH, Power PP. Lewis base induced tuning of the Ge–Ge bond order in a "digermyne". Chemical Communication. 2007;**1**:85-87

[22] Phillips AD, Wright RJ, Olmstead MM, Power PP. Synthesis and characterization of 2,6-$Dipp_2$-$H_3C_6SnSnC_6H_3$-2,6-$Dipp_2$ (Dipp = $C_6H_3$-2,6-$Pr^i_2$): A Tin analogue of an alkyne. Journal of the American Chemical Society. 2002;**124**:5930-5931

[23] Pu L, Twamley B, Power PP. Synthesis and characterization of 2,6-$Trip_2H_3C_6PbPbC_6H_3$-2,6-$Trip_2$ (Trip = $C_6H_2$-2,4,6-*i*-$Pr_3$): A stable heavier group 14 element analogue of an alkyne. Journal of the American Chemical Society. 2000;**122**:3524-3525

[24] Danovich D, Ogliaro F, Karni M, Apeloig Y, Cooper DL, Shaik S. Silynes (RC=SiR') and disilynes (RSi=SiR'): Why are less bonds worth energetically more? Angewandte Chemie International Edition. 2001;**40**:4023-4026

[25] Gau D, Kato T, Saffon-Merceron N, Cozar AD, Cossio FP, Baceiredo A. Synthesis and structure of a base-stabilized *c*-phosphino-*Si*-amino silyne. Angewandte Chemie International Edition. 2010;**49**:6585-6588

[26] Lühmann N, Müller T. A compound with a Si-C triple bond. Angewandte Chemie International Edition. 2010;**49**:10042-10044

[27] Wu P-C, Su M-D. A new target for synthesis of triply bonded plumbacetylene (RC≡PbR): A theoretical design. Organometallics. 2011;**30**:3293-3301

[28] Wu P-C, Su M-D. Effects of substituents on the thermodynamic and kinetic stabilities of HCGeX (X = H, $CH_3$, F, and Cl) isomers. A theoretical study. Inorganic Chemistry. 2011;**50**:6814-6814

[29] Wu P-C, Su M-D. Theoretical designs for germaacetylene (RC≡GeR): A new target for synthesis. Dalton Transactions. 2011;**40**:4253-4259

[30] Paetzold PI, Maisch H. Borimide, II. borimide als zwischenstufen bei der abspaltung von halogenwasserstoff aus boran-aminen. Chemische Berichte. 1968;**101**:2870-2873

[31] Paetzold PI, Stohr G. Borimide, III. borimide als dipolarophile bei der 1.3-dipolaren cyclisierungsreaktion. Chemische Berichte. 1968;**101**:2874-2880

[32] Paetzold PI, Stohr G, Maisch H, Lenz H. Borimide, IV. Die reaktion von borimiden mit phenylacetylen. Chemische Berichte. 1968;**101**:2881-2888

[33] Paetzold P, Plotho CV. Über weitere monomere borimide und ihre reaktionen. Chemische Berichte. 1982;**115**:2819-2825

[34] Geschwentner M, Eleter G, Meller A. Supermesityl-stabilisierte iminoborane. III. Zeitschrift für anorganische und allgemeine Chemie. 1993;**619**:1474-1478

[35] Gilbert TM. Ab initio computational studies of heterocycloalkynes: Structures, natural bond orders, ring strain energies, and isomerizations of cyclic iminoboranes and iminoalanes. Organometallics. 2000;**19**:1160-1165

[36] Steuber EV, Elter G, Noltemeyer M, Schmidt H-G, Meller A. First B-organyloxy-substituted iminoboranes: Preparation, stabilization, and reactivity. Organometallics. 2000; **19**:5083-5091

[37] Rivard E, Merrill WA, Wolf R, Spikes GH, Power PP. Boron–Pnictogen multiple bonds: Donor-stabilized P=B and As=B bonds and a hindered iminoborane with a B–N triple bond. Inorganic Chemistry. 2007;**46**:2971-2978

[38] Braunschweig H, Matz F, Radacki K, Schneider A. Reactivity of platinum iminoboryl complexes toward covalent element–hydrogen bonds of opposing polarity. Organometallics. 2010;**29**:3457-3462

[39] Braunschweig H, Kupfer T, Radacki K, Schneider A, Seeler F, Uttinger K, Wu H. Synthesis and reactivity studies of iminoboryl complexes. Journal of the American Chemical Society. 2008;**130**:7974-7983

[40] Dahcheh F, Stephan DW, Bertrand G. Oxidative addition at a carbene center: Synthesis of an iminoboryl–CAAC adduct. Chemistry: A European Journal. 2015;**21**:199-204

[41] Pyykko P, Desclaux J-P. Relativity and the periodic system of elements. Accounts of Chemical Research. 1979;**12**:276-281

[42] Kutzelnigg W. Chemical bonding in higher main group elements. Angewandte Chemie International Edition. 1984;**23**:272-295

[43] Pyykko P. Relativistic effects in structural chemistry. Chemical Reviews. 1988;**88**:563-594

[44] Pyykko P. Strong closed-shell interactions in inorganic chemistry. Chemical Reviews. 1997;**97**:597-636

[45] Wiberg KB. Application of the pople-santry-segal CNDO method to the cyclopropylcarbinyl and cyclobutyl cation and to bicyclobutane. Tetrahedron. 1968;**24**:1083-1096

[46] Reed AE, Curtiss LA, Weinhold F. Intermolecular interactions from a natural bond orbital, donor-acceptor viewpoint. Chemical Reviews. 1988;**88**:899-926

[47] Glendening ED, Weinhold F. Natural resonance theory: I. General formalism. Journal of Computational Chemistry. 1998;**19**:593-609

[48] Glendening ED, Weinhold F. Natural resonance theory: II. Natural bond order and valency. Journal of Computational Chemistry. 1998;**19**:610-627

[49] Glendening ED, Badenhoop JK, Weinhold F. Natural resonance theory: III. Chemical applications. Journal of Computational Chemistry. 1998;**19**:628-646